Life cycle environmental analysis of a hydrogen-based energy storage system for remote applications

Energy Reports 8 (2022) 5080–5092

Contents lists available at ScienceDirect

Energy Reports

journal homepage: www.elsevier.com/locate/egyr

Research paper

Life cycle environmental analysis of a hydrogen-based energy storage system for remote applications

David Bionaz [a], Paolo Marocco [a,*], Domenico Ferrero [a], Kyrre Sundseth [b], Massimo Santarelli [a]

[a] Department of Energy, Politecnico di Torino, Torino, Italy
[b] Sustainable Energy Technology Department, SINTEF Industry, Trondheim, Norway

ARTICLE INFO

Article history:
Received 5 November 2021
Received in revised form 1 March 2022
Accepted 23 March 2022
Available online xxxx

Keywords:
LCA
Environmental impact
Hydrogen
Renewable energy
Off-grid communities

ABSTRACT

Energy storage systems are required to address the fluctuating behaviour of variable renewable energy sources. The environmental sustainability of energy storage technologies should be carefully assessed, together with their techno-economic feasibility. In this work, an environmental analysis of a renewable hydrogen-based energy storage system has been performed, making use of input parameters made available in the framework of the European REMOTE project. The analysis is applied to the case study of the Froan islands (Norway), which are representative of many other insular microgrid sites in northern Europe. The REMOTE solution is compared with other scenarios based on fossil fuels and submarine connections to the mainland grid. The highest climate impacts are found in the diesel-based configuration (1,090.9 $kgCO_2eq/MWh$), followed by the REMOTE system (148.2 $kgCO_2eq/MWh$) and by the sea cable scenario (113.7 $kgCO_2eq/MWh$). However, the latter is biased by the very low carbon intensity of the Norwegian electricity. A sensitivity analysis is then performed on the length of the sea cable and on the CO_2 emission intensity of electricity, showing that local conditions have a strong impact on the results. The REMOTE system is also found to be the most cost-effective solution to provide electricity to the insular community. The in-depth and comparative (with reference to possible alternatives) assessment of the renewable hydrogen-based system aims to provide a comprehensive overview about the effectiveness and sustainability of these innovative solutions as a support for off-grid remote areas.

1. Introduction

Energy transition towards a low-carbon economy is a key challenge for the next decades (IPCC, 2014). The development of non-fossil fuel sources and the attempt to reduce carbon dioxide emissions are leading to an increasing penetration of renewable energy sources (RESs). RESs have recently experienced significant cost reductions and technological improvements, driven also by growing research efforts (Roy et al., 2018; Verma and Das, 2021). A considerable increase in their installed capacity is expected in the near future (Almuni et al., 2020). Electrical energy storage becomes thus crucial to overcome main issues that are associated to the fluctuating behaviour of variable RESs (VRESs), like solar and wind, and foster their penetration on a large scale (Buffo et al., 2019). Hydrogen storage represents a promising solution for large-size and long-term storage applications (International Energy Agency, 2021), which will most probably be required in the next few years when a massive RES introduction is expected (Luo et al., 2015).

Focusing on off-grid areas, diesel engines still dominate the scene of local electricity generation, despite the related environmental problems and high costs because of fuel transport. Around the world, there are more than 10,000 islands, inhabited by a total of about 750 million people. Many of them, especially those in the range from 1000 to 100,000 inhabitants, rely on diesel generators and spend a considerable share of their gross domestic product (GDP) on the import of fuels (IRENA, 2015). Thus, there is a huge global potential for incorporating renewables into mini-grids. However, electrical energy storage should be considered to enhance the exploitation of local VRESs and make the energy supply more reliable (Sawle et al., 2018). When high storage capacity is required (which is typical for off-grid renewable energy systems), batteries alone become very expensive and their hybridization with a hydrogen-based power-to-power (P2P) system can result in a cheaper solution (Marocco et al., 2021a). A H_2-based P2P system includes an electrolyzer for the conversion of the excess renewable energy into hydrogen, a pressurized vessel for the

* Corresponding author.
E-mail address: paolo.marocco@polito.it (P. Marocco).

https://doi.org/10.1016/j.egyr.2022.03.181

Nomenclature

Acronyms

AC	Alternating Current
CO_2	Carbon Dioxide
CO_2eq	Equivalent Carbon Dioxide
DG	Diesel Generator
ELY	Electrolyzer
EOL	End Of Life
EU	European Union
FC	Fuel Cell
GDP	Gross Domestic Product
GHG	Greenhouse Gases
GWI	Global Warming Impact
GWP	Global Warming Potential
H_2	Hydrogen
ICE	Internal Combustion Engine
ISO	International Standards Organization
LCA	Life Cycle Assessment
LCOE	Levelized Cost Of Energy
Li	Lithium
MILP	Mixed Integer Linear Programming
MVAC	Medium Voltage Alternating Current
NPC	Net Present Cost
OM	Operation and Maintenance
P2P	Power to Power
PEM	Proton Exchange Membrane
PV	Photovoltaic
RES	Renewable Energy Sources
RP	Replacement
SOC	State Of Charge
SS	Stainless Steel
UNFCCC	United Nations Framework Convention on Climate Change
UPS	Uninterruptible Power Supply
VRES	Variable Renewable Energy Sources
WT	Wind Turbine

Symbols

C_{inv}	Investment cost (€)
C_{OM}	Operation and maintenance cost (€/y)
C_{RP}	Replacement cost (€)
d	Real discount rate
E	Energy supplied by the system (kWh)
n	Lifetime of the project

storage of hydrogen and a fuel cell to reconvert hydrogen into electricity when required (Marocco et al., 2020).

Thus, growing attention is focusing on the analysis of hydrogen-based applications in off-grid locations (Vivas et al., 2018). Guinot et al. (2015) performed the optimal sizing of an off-grid PV-battery-hydrogen system and compared this scenario with alternative options based on diesel and batteries. They showed that the hydrogen chain has an important role in lowering the cost of the supplied energy. Marchenko and Solomin (2017) revealed that the presence of both batteries (efficient for the short-term) and hydrogen systems (cost-effective for the long-term) can result in a cost-competitive configuration. Fazelpour et al. (2016) and Homayouni et al. (2017) reported that hybridizing batteries with hydrogen can lead to the cheapest off-grid system configuration, since hydrogen reduces the need for large-size and costly batteries. The key role of hydrogen in remote areas was also demonstrated by Shahid et al. (2022), who carried out a techno-economic analysis of hydrogen-based P2P systems in small French islands at the national level. Ayodele et al. (2021) investigated an off-grid hybrid renewable energy system with hydrogen storage for a rural health clinic. They found that the hydrogen-based solution is economically preferable compared to grid extension. Gutiérrez-Martín et al. (2021) investigated the hydrogen production through water electrolysis powered by off-grid solar PV, reporting production costs of around 6 to 7 €/kg. Janssen et al. (2022) showed that the cost of off-grid renewable hydrogen could fall below 2 €/kg by 2050 in several European countries. The authors also found that a hybrid system configuration, with both solar PV and onshore wind, was the most cost-effective solution. Environmental advantages are also associated to H_2-battery P2P systems, mainly because the diesel fuel consumption can be significantly reduced (Margaret Amutha and Rajini, 2015). Groppi et al. (2018) investigated the economic and environmental sustainability of an energy system composed of a solar PV plant and a hydrogen-battery storage in the island of Favignana (Italy). They demonstrated that the hybrid storage system was a reliable option for enhancing the energy independence of small islands and decarbonizing the transport sector.

Environmental studies of hydrogen-based systems, from a life cycle assessment (LCA) perspective, have also been addressed in the literature. Zhao and Pedersen (2018) carried out a detailed LCA of a wind–hydrogen system in an isolated territory. In their study the produced hydrogen was used as a fuel for fuel cell vehicles and to provide electricity and heat through fuel cells. They showed a significant reduction in greenhouse gas (GHG) emissions compared to conventional solutions, especially when considering hydrogen for mobility purposes. Belmonte et al. (2016) performed the LCA of an off-grid hydrogen-based P2P system. For the sake of comparison, they also investigated the performance of an energy system with only batteries as a storage medium. They found that, even if the H_2 technology was more expensive than Li-ion batteries, it was characterized by a lower environmental burden. Similar considerations were derived by Belmonte et al. (2017), who analysed energy storage options based on fuel cells for stationary and mobile applications. Mori et al. (2014) assessed the environmental impacts of an uninterruptible power supply (UPS) system including hydrogen technologies and renewable energy sources. They observed that the hydrogen solution was more sustainable than a traditional UPS system based on internal combustion engine (ICE). Most of impacts of the H_2 system were due to the manufacturing phase, unlike the ICE whose operation was highly impactful due to the fuel combustion. The environmental impacts of UPS systems with fuel cells were also investigated by Stropnik et al. (2018), who highlighted the importance of circular economy in the final LCA results.

In this work, a holistic environmental analysis of a hybrid hydrogen-battery P2P system, located in the Froan Islands (Norway), is performed. The analysis is carried out in the framework of the European project REMOTE (REMOTE, 2018), whose goal is to demonstrate the techno-economic and environmental feasibility of hybrid hydrogen-battery storage systems in off-grid locations. The global warming impact (GWI) of the REMOTE system is compared with that of other scenarios based on diesel generators (Diesel case) and submarine connections (Cable case) with the mainland grid. Moreover, additional scenarios are investigated by performing a sensitivity analysis on the length of the sea cable and on the carbon intensity of electricity. The levelized cost of energy (LCOE) of each configuration is also estimated to find out

which is the most performing solution from an economic point of view. The main goal is to provide a comprehensive overview about the effectiveness of hybrid hydrogen-battery storage systems in off-grid remote areas. The thorough and comparative (with reference to possible alternatives) environmental assessment of the renewable hydrogen-battery solution represents a novelty with respect to the extant literature. The present analysis is also strengthened by the use of valuable data and experience from the REMOTE project.

2. Present situation and main scenarios

The Froan archipelago is located in a harsh environment off the west coast of Norway, near Trondheim (Marocco et al., 2020). The annual electrical load of the site is around 571 MWh, with a peak slightly higher than 100 kW. Today, the islands are connected to the mainland electric grid by means of an outdated submarine cable about to be disposed, whose total length is approximately 23.4 km. The expensive and invasive replacement of the cable suggests finding alternatives to avoid the electrical connection with the mainland. The easiest option could be the on-site installation of diesel generators. However, the high operating costs due to diesel consumption and the related pollution issues make this choice impracticable, also being the islands a nature reserve and conservation area.

The solution proposed by the REMOTE project aims to exploit local renewable energy sources (wind and solar energy) to provide a cleaner, cost-effective and reliable power supply. The inclusion of a storage system is also fundamental to manage VRES fluctuations and make this option almost totally self-sustainable. Thus, a hybrid storage solution, integrating batteries and hydrogen, was considered in the REMOTE configuration. More specifically, the REMOTE scenario, which is shown in Fig. 1a, includes a ground-mounted PV plant of 250 kW peak, 3 wind turbines (WT) of 225 kW each, a battery storage system (composed of 5 Li-ion battery racks of 110 kWh each) and the H_2-based P2P storage system. The hydrogen system consists of a PEM water electrolyzer (ELY) of 55 kW, a storage tank with capacity of 100 kg of hydrogen (operating pressure up to 30 bar) and a PEM fuel cell (FC) of 100 kW peak. A diesel generator (DG) with 100 kW nominal size was also considered as a final back-up unit, which intervenes when the renewable P2P system is not sufficient to cover the electrical load or in case of maintenance and failures in the main plant.

In the present analysis, the REMOTE solution was compared with two different scenarios: replacement of the submarine cable (Cable scenario, Fig. 1b) and installation of diesel generators to cover the entire load (Diesel scenario, Fig. 1c). It can be noted that a single 100 kW diesel generator is found in the REMOTE system. The same back-up unit was supposed for the Cable scenario, to be used in case of cable failures. Two 54 kW diesel generators were instead assumed to supply the Froan site in the Diesel scenario. The choice of using two medium generators instead of a single larger one is due to the fact that, in the Diesel scenario, gensets are required to work continuously at variable load. The efficiency of a diesel generator depends not only on the size, but also on the operating power (and decreases when working at partial loads) (Zhao et al., 2019). Moreover, if one generator needs maintenance, the system can still supply the load with the remaining genset.

Further scenarios were also investigated by varying the sea-cable length and the carbon intensity of electricity production.

3. Methodology

The environmental analysis of the different scenarios was performed in terms of global warming impact (GWI), using the carbon dioxide equivalent (CO_2eq) as emissions metric. CO_2eq has been adopted by the United Nations Framework Convention on Climate Change (UNFCCC) in its Kyoto Protocol and it is now widely used as common scale for comparing GHG emissions. It is defined as the amount of carbon dioxide emissions that would cause, over a standard 100-year time horizon, the same integrated radiative forcing of the actual emission of different greenhouse gases. More specifically, CO_2eq can be derived through the sum of all the real GHG emissions multiplied each by the respective value of 100-year global warming potential (GWP-100) (IPCC, 2014). The International Standards Organization (ISO) has defined and adopted standards that provide references for the correct application of a life cycle analysis. In this work, the environmental study of the Froan energy system was developed following the ISO standard from Refs. ISO (2006a) and ISO (2006b).

The main goal of the present analysis is to compute the GWI of the REMOTE scenario and compare it with that of the Cable and Diesel cases. The study is based on both real data from the plant and data taken from the literature. It was performed considering the entire life cycle of the plant, including extraction and processing of raw materials, manufacture, installation, use, recycling and final disposal. Transports were not considered due to the lack of data, however their contribution can be assumed to be negligible (Stropnik et al., 2018; Magrassi et al., 2019). The LCA physical boundaries are graphically displayed in Fig. 1. The local distribution grid is outside the boundaries since it is in common with all the scenarios under analysis. A plant lifetime of 25 years was considered for the LCA. In order to compare the different scenarios, the results were expressed in the same functional unit, i.e., 1 kg of CO_2eq emitted referred to 1 MWh of electricity generated onsite or supplied by the submarine cable. The final aim is to evaluate if a solution that relies on local VRESs coupled with a hydrogen-based storage system is able, and to what extent, to determine a reduction in GHG emissions (compared to more traditional solutions) when considering a full LCA perspective.

Scenarios were also compared from an economic point of view to obtain a clearer picture about the performance of hydrogen-based energy systems in remote locations.

3.1. CO_2eq emissions

The estimation of the CO_2 equivalent emissions is described below. Table 1 reports a summary of the values that have been adopted for the various subsystems.

3.1.1. PV power plant

The REMOTE PV plant consists of mono-crystalline Si solar modules. The study by Magrassi et al. (2019) was considered for the estimation of the specific CO_2eq emissions of the PV system. Their study was based on a cradle-to-grave approach with the inclusion of acquisition of raw materials, transport, manufacturing, installation, operation, maintenance and end-of-life (EOL) operations. They assumed the PV plant materials to be sent to a landfill at the EOL. In our study, the impacts related to the transport phase have been removed (whose influence is, however, negligible Magrassi et al., 2019). The resulting GHG emissions per area installed are around 304.0 $kgCO_2eq/m^2$.

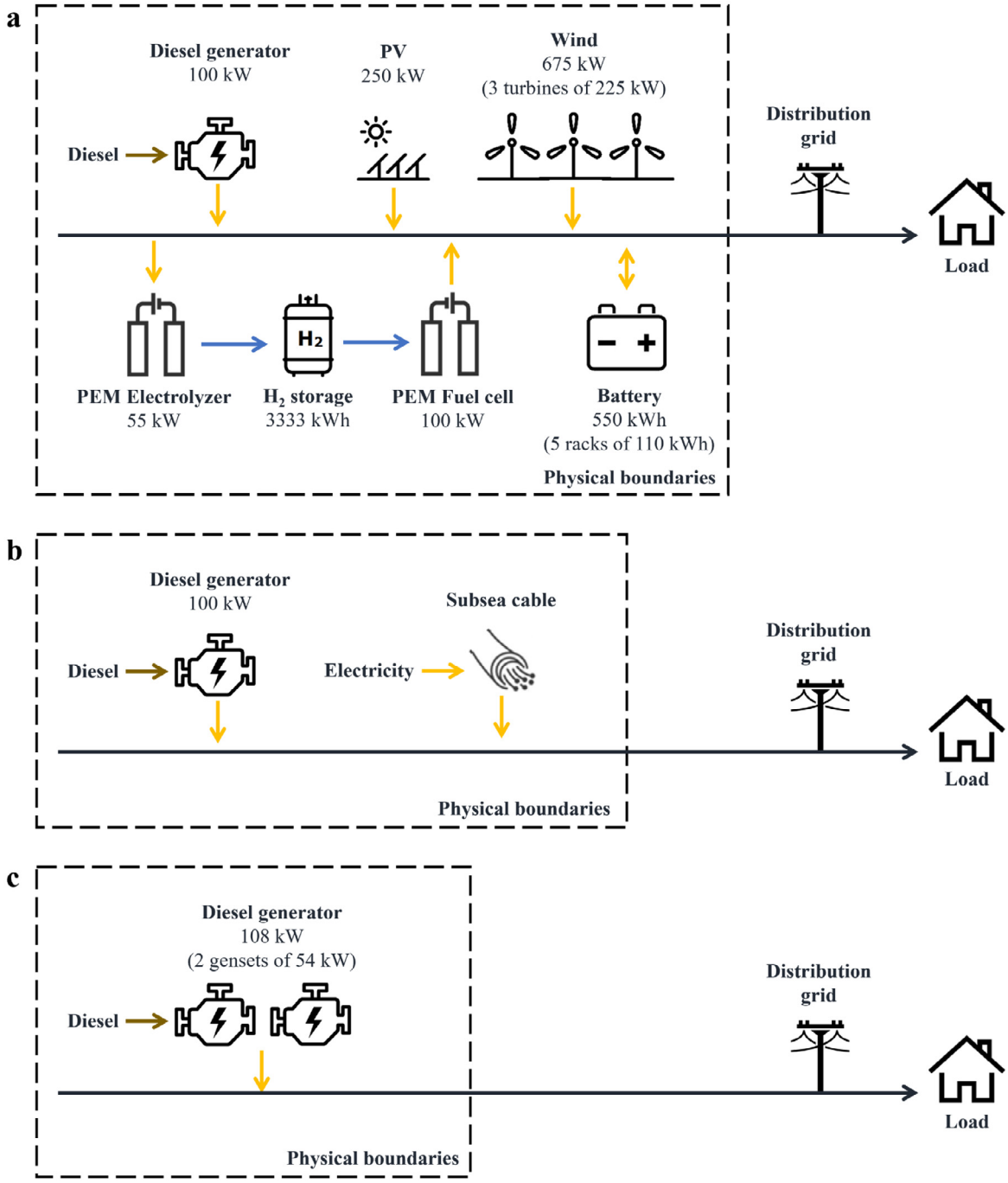

Fig. 1. Schemes of the components and of the LCA physical boundaries considered in the REMOTE (a), Cable (b), and Diesel (c) scenarios.

3.1.2. Wind power plant

Demir and Taşkin (2013) analysed the environmental impacts of wind turbines with different sizes (330, 500 and 810 kW) and hub heights (50, 80 and 100 m). Their LCA analysis included the following phases: raw material extraction, manufacturing and assembly of wind turbine components, wind turbine transportation and installation on site, operation, maintenance and EOL processes (i.e., dismantling and recycling). Contributions due to the transports could not be removed because of the lack of specific data, but they have little influence on the total emissions.

Vestas V27 turbines (225 kW and height of 33.5 m) (The Wind Power, 2021) have been selected for the Froan site. We computed their impact based on the data from Demir and Taşkin (2013). More specifically, polynomial trend curves were derived to express the GHG emissions as a function of the hub height and WT capacity. GHG emissions caused by a single V27 turbine were found to be 226,741.7 $kgCO_2eq$.

3.1.3. Li-ion battery

The work by Vandepaer et al. (2017) was considered to estimate the GHG emissions of the Li-ion battery system. They adopted an LCA cradle-to-grave approach, including extraction of raw materials, manufacture of the battery components, installation on site, maintenance and use phases, production and delivery of the stored electricity, transport and EOL treatments. Their analysis also included a metal packaging and a battery container. In our study, the GHG share related to the production/delivery of electricity was removed. The available data were not sufficient

to remove the contribution of transports from our analysis. The resulting GHG emissions per kWh of installed capacity are 130.7 $kgCO_2eq/kWh$.

3.1.4. PEM electrolyzer

GHG emissions were derived from the study by Zhang et al. (2017), who performed the LCA of a PEM electrolysis system, with also the inclusion of waste treatment and disposal phases. By removing the impact due to the electricity contribution (since it is already accounted for in the PV and WT systems), we found that GHG emissions are about 190.5 $kgCO_2eq$ per kW installed. A 20-feet container of stainless steel (SS) with total mass of 3900 kg (Bareiß et al., 2019) was also considered. Assuming an SS emission factor of 2.9 $kgCO_2eq/kgSS$ (ISSF, 2015), the container-related impacts are 11,310.0 $kgCO_2eq$.

3.1.5. PEM fuel cell

LCA data for the PEM fuel cell system were taken from Stropnik et al. (2018). The authors followed a cradle-to-grave analysis and compared three different EOL scenarios. Their landfill scenario was considered in our analysis since it is currently the most used option for fuel cell technologies (Stropnik et al., 2018). By removing the GHG contributions related to the battery and cabined components, the resulting GHG emissions per kW installed account for 405.5 $kgCO_2eq/kW$. Analogously to the PEM electrolyzer system, the impact due to a 20-feet SS container was also included (11,310 $kgCO_2eq$).

3.1.6. Hydrogen tank

The austenitic SS type 316 (EN 1.4401) was chosen as material for the storage vessel. A maximum internal pressure of 45 bar (i.e., safety factor of 1.5) was assumed. The thickness of the tank (4.0 cm) was computed by applying formula for thin-walled cylindrical pressure vessels. The hydrogen tank volume (2.9 m^3) was derived supposing it to be composed of a cylinder and two semi-spheres. The SS mass (23,386 kg) was then assessed from the SS volume and density (8.0 g/cm^3). Based on an SS emission factor of 2.9 $kgCO_2eq/kgSS$ (ISSF, 2015), GHG emissions were finally computed (67,820.6 $kgCO_2eq$). The GHG contributions due to installation, transport, operation and maintenance, and EOL process were excluded because of lack of specific data. However, their contribution is expected to be negligible compared to the SS production phase (Mori et al., 2014).

3.1.7. Diesel generator

The EU average value of 17.4 $kgCO_2eq$ per GJ of produced diesel was assumed for the fuel production phase (European Commission DG Ener, 2015). This value refers to a well-to-tank approach, from extraction up to the final consumer (with the exclusion of the combustion phase). A value of 2.9 $kgCO_2eq$ per litre of diesel burnt was hypothesized for the combustion process (Fleck and Huot, 2009), which lies in the range of 2.4 to 3.5 $kgCO_2eq/l$ reported by Jakhrani et al. (2012). Finally, the emissions related to the manufacturing of the diesel generator (including also the production of materials) account for approximately 107.7 $kgCO_2eq/kVA$ (Fleck and Huot, 2009; Dufo-López et al., 2011). The emissions associated to the production of the diesel tank and to the installation and maintenance processes were not considered in our study, due to the lack of data and as they are reported to be negligible (Fleck and Huot, 2009). A diesel density of 0.84 kg/l and a diesel energy content of 38.59 MJ/l were used for the GHG estimations (Fleck and Huot, 2009).

Table 1
CO2eq emissions of the components involved in the Froan scenarios.

Subsystem	Value
PV plant	304.0 $kgCO_2eq/m^2$
Wind plant	226,741.7 $kgCO_2eq$/turbine
Li-ion battery	130.7 $kgCO_2eq/kWh$
PEM electrolyzer	• 190.5 $kgCO_2eq/kW$ (ELY system) • 11,310 $kgCO_2eq$ (20-feet SS container)
PEM fuel cell	• 405.5 $kgCO_2eq/kW$ (FC system) • 11,310.0 $kgCO_2eq$ (20-feet SS container)
Hydrogen tank	67,820.6 $kgCO_2eq$ (capacity of 100 kg of hydrogen)
Diesel generator	• 17.4 $kgCO_2eq/GJ$ (diesel production) • 2.9 $kgCO_2eq/l$ (diesel combustion) • 107.7 $kgCO_2eq/kVA$ (DG manufacturing)
Submarine cable	• 44,676.7 $kgCO_2eq/km$[a]
Electricity from grid	• 29.2 $kgCO_2eq/MWh_{el}$ (Norway) • 432.0 $kgCO_2eq/MWh_{el}$ (EU-28)

[a]Besides this term, additional GHG emissions must be considered due to cable unavailability and power losses along the cable, which will have an impact on the DG and electricity subsystems.

3.1.8. Submarine cable

Manufacture, installation, maintenance and dismantling of the new sea cable were included in our analysis, while the disposal of the old cable was not considered (since this is in common with all the scenarios). GHG emissions per kilometre of installed cable were found to be 44,676.7 $kgCO_2eq/km$, which was derived based on the study by Birkeland (2011). The unavailability of the sea cable was also considered to estimate the amount of diesel fuel that has to be consumed by the back-up genset during periods of cable failure. An unavailability value of 0.047%/km (percentage of time) was derived based on failure rates and repair times of the subsea-cable technology. Moreover, electrical losses along the cable were also estimated to evaluate the total electricity withdrawn from the grid, i.e., net + losses. These losses were found to account for approximately 0.0645%/km (percentage of the net energy supplied by the cable). Additional information is reported in Appendix B.

3.1.9. Electricity from the mainland grid

The cable-based scenarios require the estimation of the environmental impacts caused by the production and distribution of electricity that is delivered to the Froan site through the submarine cable. The average equivalent carbon dioxide intensity of the Norwegian electricity is 29.2 $kgCO_2eq/MWh_{el}$ (ecoinvent, 2021). This very small value is due to the high renewable contribution to the Norwegian electricity production mix (98% of the total NVE, 2021). A higher GHG intensity, of about 432.0 $kgCO_2eq/MWh_{el}$, is instead reported for the European electricity mix (Moro and Lonza, 2018).

3.2. Energy simulations

Energy simulations of the Froan system have been performed over 1 reference year with hourly resolution. This was required to evaluate the data needed for the LCA analysis, such as the energy exchanges between the components and their total working hours (the latter are necessary to estimate the component lifetimes). The HyOpt tool was employed to perform the energy simulation and determine the cost-optimal operation of the system. It is an optimization model developed by SINTEF Industri (SINTEF, 2022) for the design and evaluation of energy systems, including hydrogen-based technologies. HyOpt consists of three parts: an Excel front end where the required input parameters can be specified, a SQLite database, and the optimization

Table 2
Main technical parameters of the components involved in the Froan scenarios.

Component	Value
PV plant	
Rated power	250 kW
PV panel area	1571.8 m^2
Lifetime	25 y
Wind plant	
Rated power	675 kW (3 of 225 kW each)
Hub height	33.5 m
Lifetime	25 y
Li-ion battery	
Capacity	550 kWh (5 of 110 kWh each)
Minimum SOC	0.2 (Marocco et al., 2018)
Maximum SOC	0.9 (Marocco et al., 2018)
Charging efficiency	0.96 (Marocco et al., 2018)
Discharging efficiency	0.96 (Marocco et al., 2018)
Lifetime	15 y (Vandepaer et al., 2017)
PEM electrolyzer	
Rated power	55 kW
Modulation range (% of rated power)	10 to 100% (Marocco et al., 2020)
Avg. efficiency (LHV basis)	63% (Marocco et al., 2018)
Lifetime	67,000 h (Zhang et al., 2017)
PEM fuel cell	
Rated power	100 kW
Modulation range (% of rated power)	6 to 100% (Marocco et al., 2020)
Avg. efficiency (LHV basis)	50% (Marocco et al., 2018)
Lifetime	40,000 h (Shehzad et al., 2019)
Hydrogen tank	
Capacity	100 kg (41 m^3)
Minimum SOC	0.1 (Marocco et al., 2021a)
Maximum SOC	1 (Marocco et al., 2021a)
Lifetime	25 y
Diesel generator	
Rated power	100 kW (125 kVA)[a] (Honny Power, 2021) 108 kW (134 kVA)[b] (Kohler, 2021) (2 of 54 kW each)
Fuel consumption	Avg. fuel consumption of 220 g/kWh[a] (Mori et al., 2014) Fuel consumption curve[b] (Kohler, 2021)
Lifetime	20,000 h (Jakhrani et al., 2012)

[a]REMOTE and Cable scenarios.
[b]Diesel scenario.

model itself, which is written in the FICO™ Mosel language. The optimization framework is based on the Mixed Integer Linear Programming (MILP) technique and the detailed mathematical formulation can be found in the report by Kaut et al. (2020). The objective function, which is minimized by the model, is the net present cost (NPC) of the system, whose expression is described by Eq. (A.2) in Appendix A.

Main technical data of the components involved in the Froan scenarios are summarized in Table 2. The hourly profiles of VRES supply and load demand in Froan were taken from Marocco et al. (2018). Economic assumptions are reported in Appendix A (see Table A.1).

4. Results and discussion

4.1. REMOTE scenario

Results from the energy simulation of the REMOTE system are listed in Table 3. The yearly working hours of the FC, ELY and DG were compared with their lifetime values reported in Table 2. No replacements are needed for all the three components. Similarly, no replacements are needed for the PV plant, the wind farm and the hydrogen storage tank, since their lifetimes were assumed to be equal to the duration of the project (i.e., 25 years). The batteries, instead, should be replaced once during the 25-years period, since their lifetime is assumed to be 15 years (Vandepaer et al., 2017).

Table 3
Total energy/hydrogen exchanges and working hours of all the REMOTE components over 1 reference year. Values have been derived using the optimization model HyOpt.

Subsystem	Value
PV plant	
Directly to the load	58.7 MWh/y
To the storage system	46.3 MWh/y
Curtailed	90.5 MWh/y
Wind plant	
Directly to the load	263.7 MWh/y
To the storage system	260.2 MWh/y
Curtailed	790.6 MWh/y
Hydrogen system (ELY + storage tank + FC)	
Energy from VRES (PV+wind) to ELY	105.6 MWh/y
ELY working hours	2472.5 h/y
H_2 to/from the storage tank	1920.0 kg/y
Energy from FC to the load	35.2 MWh/y
FC working hours	768.5 h/y
Battery	
Energy from VRES (PV+Wind)	200.9 MWh/y
Energy to the load	185.2 MWh/y
Diesel generator	
Energy to load	28.6 MWh/y
Working hours	438.0 h/y
Total load	
Total energy (VRES+storage+diesel) to the load	571.3 MWh/y

Based on the outcomes derived by the energy simulation and on the GHG emissions data reported in Section 3, the life cycle environmental impacts were computed for all the subsystems of the REMOTE scenario. Impacts were also divided by the total energy provided to the load over the 25-year lifetime (14,282.4 MWh) in order to express them according to the chosen functional unit. Below, results are shown for the various REMOTE components.

- **PV power plant:** The total PV-related environmental impacts are approximately 477,813.1 $kgCO_2eq$ and, in functional unit, 33.5 $kgCO_2eq/MWh$. Based on the REMOTE plant simulation, GHG emissions were also normalized to the energy produced by the PV panels, both in case of real production (182.0 kgCO2eq/MWh) and in the ideal case with no curtailments (97.8 kgCO2eq/MWh). These values lie in the range of 29.0 to 671.0 kgCO2eq/MWh reported by Ludin et al. (2018) for the mono-crystalline Si technology.
- **Wind power plant:** The resulting GHG emissions of the three wind turbines are 680,225.1 $kgCO_2eq$ and, in functional unit, 47.6 $kgCO_2eq/MWh$. In order to compare our results with other values from literature, we normalized the total CO_2eq by the energy that is produced only by the wind turbines both in case of real production (51.9 $kgCO_2eq/MWh$) and in the ideal case with no curtailments (20.7 $kgCO_2eq/MWh$). These results are in agreement with the large range of GHG emissions of WT systems found in literature (from 1.7 to 123.7 $kgCO_2eq/MWh$) (Demir and Taşkin, 2013; Wang and Sun, 2012; Varun et al., 2009; Dolan and Heath, 2012; Raadal et al., 2011).
- **Li-ion battery:** The total GHG emissions (with inclusion of the GWI share due to replacement) are 143,803.0 $kgCO_2eq$ and, in functional unit, 10.1 $kgCO_2eq/MWh$. We also computed the mass of CO_2eq emitted per energy delivered by the batteries (31.1 $kgCO_2eq/MWh$). This value is in line with GHG emissions rates of Li-ion batteries stated by Vandepaer et al. (2017) (20.5 to 34.0 $kgCO_2eq/MWh$), by Hiremath et al. (2015) (25.0 to 49.0 $kgCO_2eq/MWh$) and by Wang et al. (2018) (16.1 to 27.8 $kgCO_2eq/MWh$).
- **PEM electrolyzer:** By summing the impacts of the ELY system (10,474.8 $kgCO_2eq$) and of the container (11,310.0 $kgCO_2eq$), the total GHG emissions are 21,784.8 $kgCO_2eq$ and, in functional unit, 1.5 $kgCO_2eq/MWh$.
  The emissions per H_2 produced (3.8 gCO_2eq/MJ_{H2}) were also derived. They are difficult to compare with literature data since the ELY part is usually not separated from the electricity production system. However, the ELY impacts of our study are of the same order of magnitude of those reported by Zhang et al. (2017) (1.2 gCO2eq/MJH2) and Bareiß et al. (2019) (1.8 to 3.3 gCO2eq/MJH2). It can be noted that the REMOTE electrolyzer has a higher specific value, mainly because hydrogen is here produced for storage purposes, i.e., only when VRES surplus energy occurs (which means higher values of normalized GHG emissions).
- **PEM fuel cell:** The total GHG emissions of the FC system are 51,858.3 $kgCO_2eq$, of which 40,548.3 $kgCO_2eq$ are due to the FC and 11,310.0 $kgCO_2eq$ to the 20-feet container. The total value, in functional unit, is around 3.6 $kgCO_2eq/MWh$.
  The ratio of the total GHG emissions to the energy delivered by the FC was also computed, resulting in a value of 59.0 $kgCO_2eq/MWh$. This value is more than 4 times higher than that reported by Mori et al. (2014) (13.4 $kgCO_2eq/MWh$). The reason is because in the work by Mori et al. (2014), an UPS system working continuously during its lifetime was considered. In the REMOTE plant, instead, the fuel cell produces energy only when the VRES electricity is not sufficient to cover the load. If we consider an ideal case where the REMOTE FC operates without interruption at constant rated power, the specific GHG emissions become approximately 13.0 $kgCO_2eq/MWh$, which is very close to the value reported by Mori et al. (2014).
- **Hydrogen tank:** The total environmental impacts associated to the SS storage tank are 67,820.6 $kgCO_2eq$ and, in functional unit, 4.7 $kgCO_2eq/MWh$. The SS mass of our tank (23,386.4 kg) is higher than that of the storage analysed by Mori et al. (2014), because of the higher pressure and volume capacity of the REMOTE storage system. However, even though the mass of the REMOTE tank is greater, the final GHG impacts are slightly lower. This is due to the higher emission factor (4.5 kgCO2eq/kgSS) that was assumed by Mori et al. (2014).
- **Diesel generator:** The fuel consumption derived by the simulation is 7481.3 litres per year. Over the lifetime of the project, the total GHG emissions of the diesel generator account for around 673,965.8 $kgCO_2eq$ and, in functional unit, 47.2 $kgCO_2eq/MWh$. The diesel combustion is responsible for the biggest part (79.4%), followed by the fuel production (18.6%) and by the manufacture of the generator (2.0%), which is in agreement with the GHG repartition reported by Alsema (2000). DG emissions were also normalized to the energy delivered by the generator, resulting in 0.9 $kgCO_2eq/kWh$. This value is close to GHG emission outcomes of other studies: 1.3 $kgCO_2eq/kWh$ (Dufo-López et al., 2011; Alsema, 2000), 1.7 $kgCO_2eq/kWh$ (Fleck and Huot, 2009), 0.7 $kgCO_2eq/kWh$ (Smith et al., 2015) and 0.4 to 3.2 $kgCO_2eq/kWh$ (Jakhrani et al., 2012).

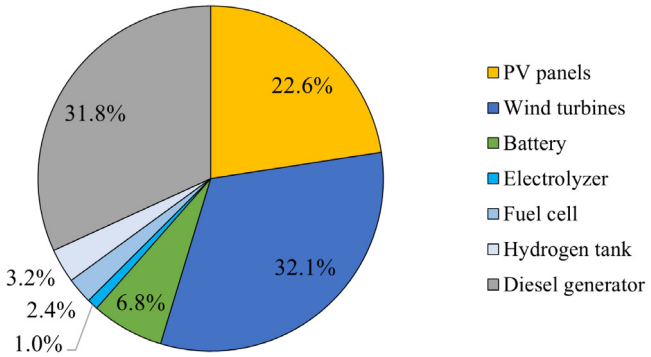

Fig. 2. Relative contributions of each subsystem to the total GHG emissions of the REMOTE scenario.

The resulting GHG emissions rates, in functional unit, of each component and of the complete REMOTE scenario are summarized in Table 4. The relative contributions of each subsystem are instead displayed in Fig. 2. Renewable generators (i.e., PV and WT) have the biggest GWI (54.7% in total). Moreover, even if the diesel generator provides only about 5% of the total energy, it has the second highest share of GHG emissions (31.8%). The storage systems have instead a lower environmental impact (13.5% in total), of which battery has a share slightly higher than the hydrogen system (6.8% compared to 6.7%).

4.2. Cable scenario

This alternative scenario (Fig. 1b) consists in the substitution of the existing outdated submarine cable that connects the Froan islands to the mainland grid. The yearly electrical load (i.e., 571.3 MWh/y) is mostly covered by the electricity supplied through the cable (565.0 MWh/y), except for a small fraction (6.3 MWh/y) that is provided by the 100-kW diesel generator. The DG intervention

Table 4
Life cycle environmental impacts (in functional unit) of each subsystem and of the energy system in the REMOTE, Cable and Diesel scenarios.

Subsystem	REMOTE scenario [$kgCO_2eq/MWh$]	Cable scenario [$kgCO_2eq/MWh$]	Diesel scenario [$kgCO_2eq/MWh$]
PV plant	33.5	–	–
Wind plant	47.6	–	–
Li-ion battery	10.1	–	–
PEM electrolyzer	1.5	–	–
PEM fuel cell	3.6	–	–
Hydrogen tank	4.7	–	–
Diesel generator	47.2	11.1	1090.9
Submarine cable	–	73.3	–
Electricity	–	29.3	–
Total	**148.2**	**113.7**	**1090.9**

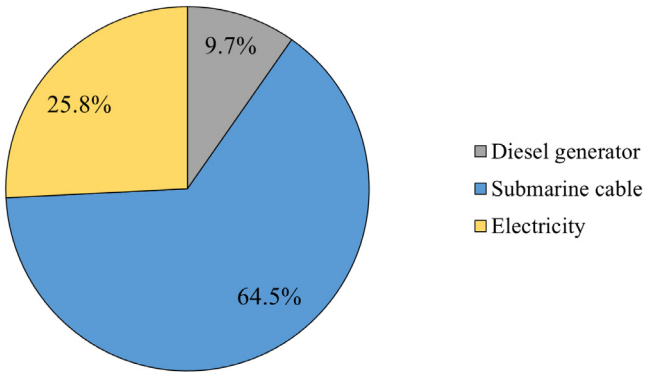

Fig. 3. Relative contributions of each subsystem to the total GHG emissions of the Cable scenario.

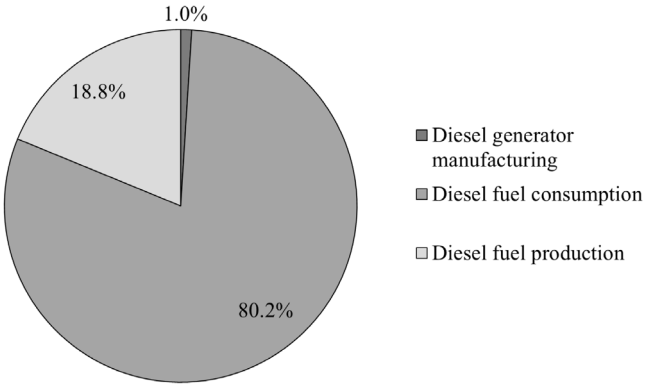

Fig. 4. Relative contributions of each DG phase to the total GHG emissions of the Diesel scenario.

is required to enhance the reliability of the energy system and satisfy the load in case of unavailability of the submarine cable. Given that the cable length is 23.4 km, the resulting cable unavailability is approximately 1.1% of the time. The diesel generator should work for about 96 hours per year, consuming 1637.3 litres of diesel fuel per year. This results in no need for DG replacement over the 25-years period (the yearly working hours of the DG were compared to its total number of life hours).

Electrical losses along the cable were also considered. The total energy that is withdrawn from the mainland grid by the subsea cable is 573.6 MWh/y, which is 1.5% higher than the net energy supplied to Froan through the cable.

The resulting GHG emissions of the Cable scenario, in functional unit, are reported in Table 4. Fig. 3 shows instead the breakdown of the GHG emissions among the three main subsystems. Almost two-thirds of the environmental impacts are caused by the submarine cable, followed by the Norwegian electricity and by the diesel generator. It can be noted that, even though the DG component covers a very small fraction of the electrical load, its contribution accounts for around 10% of the total GHG emissions.

4.3. Diesel scenario

As previously reported, two 58 kW diesel generators were considered to cover the electrical load of the Froan site. Simulations revealed that each genset is required to work approximately 8616 hours per year, meaning that each DG unit should be replaced almost every two and a half years (life hours before replacement were assumed to be 20,000 (Jakhrani et al., 2012)). By considering the fuel consumption curve from Kohler (2021), it was found that the overall diesel that is burnt accounts for 174,682.2 litres per year.

The total GHG emissions are 623,240.2 kgCO2eq/y, which, in functional unit, become 1090.9 kgCO2eq/MWh. The breakdown of the GHG emissions is similar to that found in the REMOTE scenario referring to the DG component. As shown in Fig. 4, most of the environmental impact is caused by the fuel consumption, which is responsible for 80.2% of the total emissions. The diesel fuel production phase is the second biggest contribution (18.8%), whereas the share of the DG manufacture is almost negligible (1.0%) even though a high number of DG replacements occurs over the project lifetime.

GHG emissions were also normalized to the electrical energy provided by the DG units. The resulting value is 1.1 $kgCO_2eq/kWh$, which is in line with what stated in Section 4.1 for the diesel generator.

4.4. Comparison of the scenarios

Main results of the three scenarios are summarized in Table 4. The diesel-based case has a very high GWI compared to the other scenarios, more than 7 times the impacts of the REMOTE case. Over the entire lifetime of 25 years, the installation of the renewable-fed P2P plant allows about 13,463.7 tonnes of CO_2eq to be avoided compared to the Diesel scenario. However, the Cable scenario was found to be the most environmentally-friendly solution, showing lower GHG emissions than the REMOTE case (23% less), which is due to different reasons. Firstly, the annual load coverage by diesel generators is higher in the REMOTE scenario (5.0%) than in the Cable case (1.1%). The relatively small distance of the Froan islands from the mainland is another parameter with high influence on the overall GHG emissions. The carbon intensity of the electricity transmitted by the cable has also a relevant impact on the results. Since the Norwegian electricity

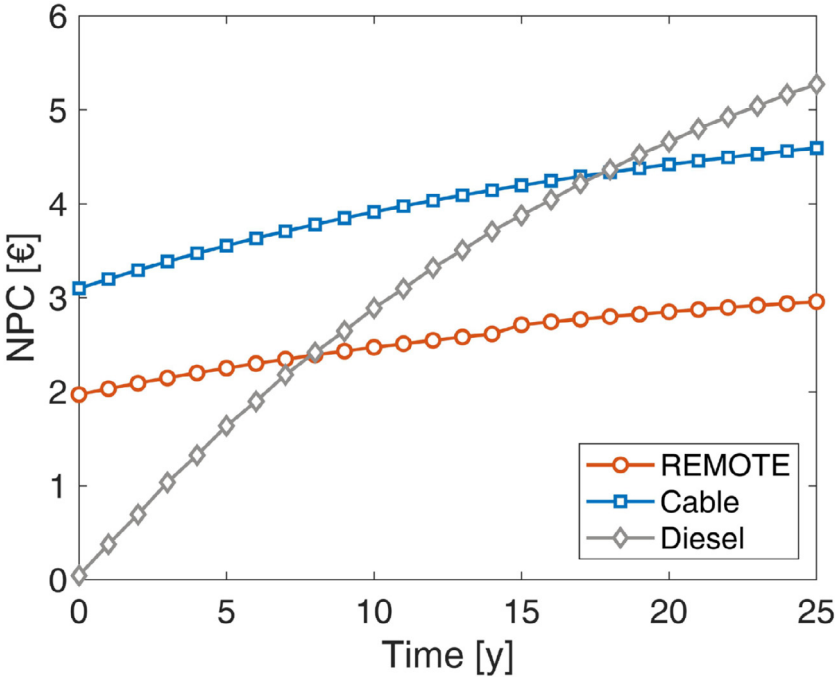

Fig. 5. NPC as a function of time for the REMOTE, Cable and Diesel scenarios.

Table 5
NPC and LCOE values at 25-year time horizon for the REMOTE, Cable and Diesel scenarios.

Parameter	REMOTE scenario	Cable scenario	Diesel scenario
NPC	2.96 M€	4.59 M€	5.27 M€
LCOE	0.37 €/kWh	0.58 €/kWh	0.66 €/kWh

production is almost totally renewable, the resulting GHG emissions are very low. These considerations show that site-specific parameters can significantly affect the results of environmental studies. In order to better generalize the obtained results, in Section 4.5 further scenarios will be investigated, performing a sensitivity analysis on the submarine cable length and on the CO_2 emission intensity of electricity.

The performance of the three scenarios was also analysed from an economic point of view. The methodology for the estimation of the economic parameters is reported in Appendix A. The resulting net present cost (NPC) and levelized cost of energy (LCOE) values are listed in Table 5, referring to the 25-year time horizon. It can be noted that the REMOTE case is the most-cost effective solution with an LCOE around 36% and 44% lower than the Cable and Diesel scenarios, respectively.

The NPC as a function of the time horizon is displayed in Fig. 5. The DG scenario is characterized by a very low investment at the beginning of the simulation. However, the high operating costs to run the DG system cause the NPC to increase sharply over the lifetime of the project. On the contrary, most of costs of the REMOTE and Cable cases are due to the high initial investment because of the renewable P2P system (REMOTE) and connection to the mainland grid (Cable). It can be noted that the REMOTE configuration is always cheaper that the cable-based case. It also becomes more attractive than the Diesel scenario after around 8 years.

4.5. Sensitivity analysis

The length of the submarine cable was varied from zero up to twice the current length. Main results are displayed in Fig. 6, where it is also shown the REMOTE case for the sake of comparison. Changing the cable length affects all subsystems involved in the Cable scenario. Firstly, the GHG emissions strictly related to the submarine cable increase linearly with increasing distance, since they have been expressed per unit of cable length, as reported in Table 1. Moreover, a longer connection also implies an increase in the cable unavailability, which entails a higher amount of DG operating hours to cover the electrical demand not satisfied by the grid, with consequent higher environmental impacts due to the diesel fuel combustion. Finally, a longer length also leads to an increase in the electrical losses along the cable, as described in Section 3.1.8.

As shown in Fig. 6, the length at which there is the GWI parity with the REMOTE case is around 1.4 times longer than the reference distance (derived by the intersection of the GHG emissions of the Cable case with the REMOTE red dashed line). When doubling the cable distance, the total GWI (197.2 $kgCO_2eq/MWh$) is 73.5% higher than that of the original Cable scenario, thus showing that the length parameter has a considerable influence on the environmental impact of the energy system. Moreover, 33.1% more emissions are produced by the double-length cable scenario compared to the REMOTE case.

It can be observed that the electricity contribution (yellow area in Fig. 6) is about constant along the length interval under analysis. This is because, by increasing the length of the cable, the electricity contribution tends to decrease due to the higher unavailability of the cable. But this is roughly balanced by the higher amount of electricity that is needed to cope with the increased losses along the cable (due to the longer length).

The influence of the carbon intensity of electricity was also investigated. More specifically, the average GHG intensity of the European electricity mix was considered. As stated in Section 3.1.9, this value accounts for 432 $kgCO_2eq/MWh$ (ecoinvent, 2021), which is almost 15 times higher than that of the Norwegian electricity (very low due to the high share of renewable sources). Main results of the Cable-EU scenarios are reported in Fig. 7 as a function of the length of the submarine cable. Unlike the Norwegian case, it can be noted that electricity is the dominant contribution over the entire length range because of the high CO_2

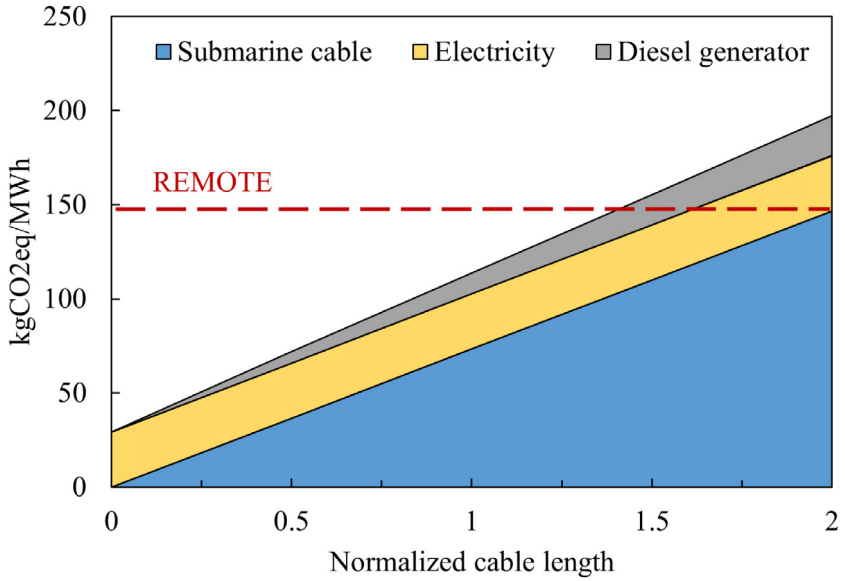

Fig. 6. GHG emissions in the Cable-Norway scenarios as a function of the length of the subsea cable (on the x-axis, the cable length is normalized to the reference length of 23.4 km).

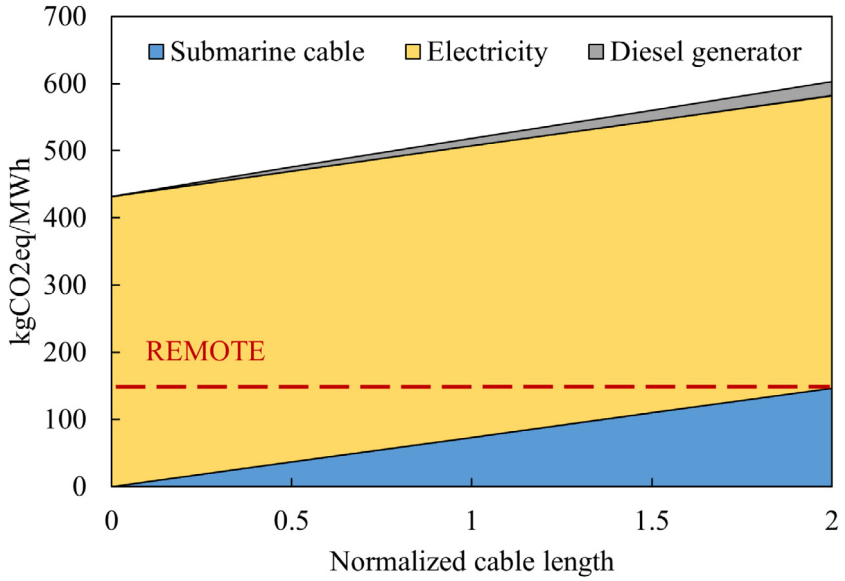

Fig. 7. GHG emissions in the Cable-EU scenarios as a function of the length of the subsea cable (on the *x*-axis, the cable length is normalized to the reference length of 23.4 km).

emission intensity of the EU electricity. Concerning the Cable-EU scenario with reference length of 23.4 km, the total GHG emissions are 518.1 $kgCO_2eq/MWh$, of which 83.7% is due to electricity and the remaining fraction to the cable (14.1%) and to the diesel generator (2.1%). It is noteworthy that this value is 249.6% higher than the GWI of the REMOTE scenario. Overall, the environmental impacts of the REMOTE system are always lower than those of the Cable-EU scenarios, regardless of the length of the submarine connection.

5. Conclusions

The present study performed an environmental analysis of a renewable hydrogen-based system, located in the Froan archipelago (Norway). This solution was compared to alternative scenarios based on diesel generators and on the replacement of the outdated sea cable to provide a clearer picture about the effectiveness and sustainability of hydrogen-based P2P systems in off-grid environments.

GHG emissions of the REMOTE scenario are 148.2 $kgCO_2$ eq/MWh, of which the renewable power plants (PV and wind) account for more than half of the impacts. Although the diesel generator only covers about 5% of the electrical load, it is responsible for approximately 31.8% of the GWI. The battery and hydrogen storage systems have the lowest environmental impact, with about 6.8% and 6.7% of the total REMOTE emissions, respectively. The Cable scenario was found to have a slightly lower impact than the REMOTE solution (113.7 $kgCO_2eq/MWh$),

Table A.1
Main economic input parameters for the estimation of the LCOE.

Component	Investment	Replacement	OM	Ref.
PV plant	1547 €/kW	–	24 €/kW/y	Marocco et al. (2020)
Wind plant	1175 €/kW	–	3%/y of Inv. cost	Marocco et al. (2020)
Li-ion battery	500 €/kWh	50% of Inv. Cost (15 y)	10 €/kWh/y	Vandepaer et al. (2017), Tsiropoulos et al. (2018)
PEM fuel cell	1978 €/kW	35% of Inv. Cost (40,000 h)	3%/y of Inv. cost	Marocco et al. (2020), Shehzad et al. (2019), Tractebel and Hinicio (2017) and Battelle Memorial Institute (2016)
PEM electrolyzer	4600 €/kW	35% of Inv. Cost (67,000 h)	3%/y of Inv. cost	Marocco et al. (2020), Zhang et al. (2017), Tractebel and Hinicio (2017) and Proost (2019)
H2 storage	470 €/kg	–	2%/y of Inv. cost	Marocco et al. (2021a)
Diesel generator	420 €/kW	420 €/kW (20,000 h)	2 €/L	Jakhrani et al. (2012) and Gracia et al. (2018)

due to the short distance from the mainland and to the very low carbon intensity of the Norwegian electricity, whose production is almost entirely renewable. The Diesel scenario has the highest GWI, which is more than 7 times higher than that of the REMOTE case, mainly because of the on-site diesel combustion (80.2% of the total emissions). An economic analysis was also carried out, showing that the REMOTE system is the most cost-effective solution. This is due to the high operating costs related to the fuel consumption (Diesel scenario) and to the capital-intensive initial cost to provide a connection to the main grid (Cable scenario).

Additional scenarios were also investigated to better evaluate the influence of the cable length and of the electricity carbon intensity. By increasing the distance from the mainland, GHG emissions increase and the cable-based case achieves the same impacts as the REMOTE system at a cable length 1.4 times longer than the reference one (whose value is 23.4 km). The carbon intensity of electricity has also a significant effect on the LCA results. In fact, when considering the European electricity mix, the GWI of the cable-based case (with reference length) becomes about 249.6% higher than that of the REMOTE scenario.

To sum up, stand-alone H_2-battery energy systems can represent a very promising solution, both from an economic and environmental point of view, compared to more traditional configurations based on fossil fuels or grid connections. LCA results are also highly influenced by parameters such as the length of the electrical connection and the carbon intensity of the mainland electricity.

Future steps will involve the implementation of the proposed LCA methodology within a multi-objective optimization framework to carry out the optimal design of hybrid energy storage systems, taking into account both economic and environmental issues.

CRediT authorship contribution statement

David Bionaz: Conceptualization, Methodology, Data curation, Writing – original draft, Visualization, Writing – review & editing. **Paolo Marocco:** Methodology, Data curation, Writing – original draft, Visualization, Writing – review & editing, Supervision. **Domenico Ferrero:** Data curation, Writing – original draft, Writing – review & editing, Supervision. **Kyrre Sundseth:** Conceptualization, Resources, Data curation, Writing – review & editing, Supervision. **Massimo Santarelli:** Writing – review & editing, Supervision, Project administration, Funding acquisition.

Declaration of competing interest

The authors declare that they have no known competing financial interests or personal relationships that could have appeared to influence the work reported in this paper.

Acknowledgments

This project has received funding from the Fuel Cells and Hydrogen 2 Joint Undertaking (now Clean Hydrogen Partnership) under Grant Agreement No 779541. This Joint Undertaking receives support from the European Union's Horizon 2020 Research and Innovation programme, Hydrogen Europe and Hydrogen Europe Research.

The authors want to thank the REMOTE project partners for their contributions in terms of input data for the modelling. We would like to thank the end user of the demonstration site in Norway (TrønderEnergi) and the power-to-power system developers (Ballard Power Systems Europe, Hydrogenics and Powidian).

Appendix A. Economic analysis

For the sake of completeness, the levelized cost of energy (LCOE) of the REMOTE scenario was computed to evaluate its cost-effectiveness compared to the Cable and Diesel cases. Main economic assumptions for the REMOTE and Diesel scenarios are reported in Table A.1. Economic parameters referred to the Cable case were instead derived from Marocco et al. (2020), based on data from TrønderEnergi (2021) (however cost details are not shown due to confidentiality issues).

Based on data in Table A.1 and outcomes from the energy simulation, the LCOE was computed according to the following relationship (Marocco et al., 2021b):

$$LCOE = \frac{NPC}{\sum_{j=1}^{n} \frac{E_j}{(1+d)^j}} \tag{A.1}$$

where NPC (in €) is the net present cost, E_j (in kWh) is the energy supplied by the system during the j-th year, n is the lifetime of the project (25 years) and d is the real discount rate (set to 4.9% (Marocco et al., 2020)). The NPC was derived as follows (Kaut et al., 2020):

$$NPC = C_{inv,0} + \sum_{j=1}^{n} \left[\frac{C_{OM,j}}{(1+d)^j} + \frac{C_{RP,j}}{(1+d)^j} \right] \tag{A.2}$$

where $C_{inv,0}$ (in €) accounts for the capital expenditures occurring at the beginning of the analysis period, $C_{OM,j}$ (in €/y) is the operation and maintenance (OM) cost of the system in the j-th year and $C_{RP,j}$ (in €) is the total replacement cost in the j-th year. The latter term is due to the periodic replacement of components (i.e., battery, H2 equipment and diesel generator) over the lifetime of the project.

The LCOE breakdown of the REMOTE scenario at the end of the project lifetime (i.e., 25 years) is shown in Fig. A.1. It can be noted that more than half of the cost share is given by the renewable generators (PV and WT), of which the highest cost fraction is due to the wind farm. The second major contributor is represented by the hydrogen equipment, which accounts for around 24% of the total LCOE. Finally, the battery and the diesel generator units are responsible for 14% and 9% of the cost, respectively.

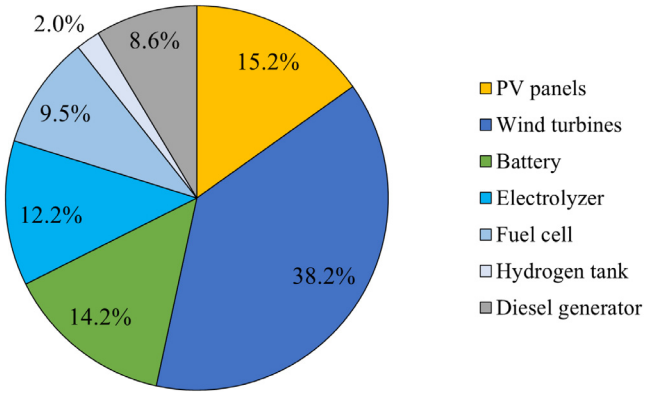

Fig. A.1. LCOE breakdown at 25-year time horizon for the REMOTE scenario.

Appendix B. Additional information about the submarine cable subsystem

A three-core medium-voltage AC (MVAC) submarine cable, with nominal voltage of 10 kV, has been considered (Nexans, 2021). Each core includes a conductor section and an insulation layer, made of cross-linked polyethylene (XLPE).

LCA data for the cable were taken from Birkeland (2011), who carried out an LCA of 33-kV three-core sea cables (with copper as conductor and XLPE as insulator). They considered a cable length of 63.3 km and assumed a lifetime expectancy of 40 years. Their analysis included the manufacturing phase, transports, installation of the cables (laid and buried one metre into the seabed), their inspection and maintenance during operation, dismantling and EOL phases. In our study, in accordance to the chosen LCA boundaries, the contribution due to transports was not considered. The impact related to the maintenance was also scaled down to the assumed 25-years lifetime. The GHG emissions per cable mass from Birkeland (2011) account for about 1.74 $kgCO_2eq/kg$, which is very similar to the value reported by Yang et al. (2018) (1.658 $kgCO_2eq/kg$) and Nian et al. (2019) (1.665 $kgCO_2eq/kg$). Based on this value, the GWI of the manufacture phase was evaluated per kilometre of cable, considering that the specific weight of the cable under analysis is approximately 9.9 t/km (Nexans, 2021). The resulting GWI breakdown of the submarine cable is as follows: 39.4% for the operation of the cable (including maintenance and inspection), 38.6% due to the cable manufacture, 11.5% because of installation, and finally 10.5% for the dismantling process.

The unavailability of the submarine cable technology was also estimated. This has an impact on the GWI of the energy system since diesel generators should intervene during failure periods, with consequent GHG emissions (mainly due to the fuel combustion process). Concerning the reliability of MVAC submarine cables, the failure rates and related repair times were taken from Warnock et al. (2019) and Karlsdóttir (2013). More specifically, Warnock et al. (2019) presented a review of submarine transmission failures in European offshore wind farms and reported a mean failure rate of 0.00299 failures/km/year when considering 10–66 kV MVAC cables. The repair of a submarine cable damage involves several activities with different durations. A total repair time of 57 day (Karlsdóttir, 2013), referred to the North Sea, was considered in this analysis.

Finally, the electrical losses along the cable have to be computed for an estimation of the total electricity withdrawn from the mainland grid. These losses are around 0.0645%/km (percentage of the net energy supplied by the cable). They were derived considering a conductor section of 70 mm^2 with a resistance of 1.02 Ω/km (Nexans, 2021).

References

Almuni, M., Dauwe, T., Moorkens, I., Saarikivi, R.J., Tomescu, M., 2020. Renewable energy in Europe - 2020. Recent growth and knock-on effects.

Alsema, E.A., 2000. Environmental life cycle assessment of solar home systems.

Ayodele, T.R., Mosetlhe, T.C., Yusuff, A.A., Ogunjuyigbe, A.S.O., 2021. Off-grid hybrid renewable energy system with hydrogen storage for South African rural community health clinic. Int. J. Hydrog. Energy 46 (38), 19871–19885. http://dx.doi.org/10.1016/j.ijhydene.2021.03.140.

Bareiß, K., de la Rua, C., Möckl, M., Hamacher, T., 2019. Life cycle assessment of hydrogen from proton exchange membrane water electrolysis in future energy systems. Appl. Energy 237 (January), 862–872. http://dx.doi.org/10.1016/j.apenergy.2019.01.001.

Battelle Memorial Institute, 2016. Manufacturing cost analysis of PEM fuel cell systems for 5- and 10-kW backup power applications.

Belmonte, N., Luetto, C., Staulo, S., Rizzi, P., Baricco, M., 2017. Case studies of energy storage with fuel cells and batteries for stationary and mobile applications. Challenges 8 (1), 9. http://dx.doi.org/10.3390/challe8010009.

Belmonte, N., et al., 2016. A comparison of energy storage from renewable sources through batteries and fuel cells: A case study in Turin, Italy. Int. J. Hydrog. Energy 41 (46), 21427–21438. http://dx.doi.org/10.1016/j.ijhydene.2016.07.260.

Birkeland, C., 2011. Assessing the Life Cycle Environmental Impacts of Offshore Wind Power Generation and Power Transmission in the North Sea. NTNU.

Buffo, G., Marocco, P., Ferrero, D., Lanzini, A., Santarelli, M., 2019. Power-to-x and power-to-power routes. In: Solar Hydrogen Production. pp. 529–557.

Demir, N., Taşkin, A., 2013. Life cycle assessment of wind turbines in pinarbaşI-Kayseri. J. Clean. Prod. 54, 253–263. http://dx.doi.org/10.1016/j.jclepro.2013.04.016.

Dolan, S.L., Heath, G.A., 2012. Life cycle greenhouse gas emissions of utility-scale wind power: Systematic review and harmonization. J. Ind. Ecol. 16 (SUPPL.1), http://dx.doi.org/10.1111/j.1530-9290.2012.00464.x.

Dufo-López, R., et al., 2011. Multi-objective optimization minimizing cost and life cycle emissions of stand-alone PV-wind-diesel systems with batteries storage. Appl. Energy 88 (11), 4033–4041. http://dx.doi.org/10.1016/j.apenergy.2011.04.019.

ecoinvent, 2021. ecoinvent database. [Online]. Available: https://ecoinvent.org/the-ecoinvent-database/ [Accessed: 04-Oct-2021].

European Commission DG Ener, 2015. Study on actual GHG data for diesel, petrol, kerosene and natural gas.

Fazelpour, F., Soltani, N., Rosen, M.A., 2016. Economic analysis of standalone hybrid energy systems for application in Tehran, Iran. Int. J. Hydrog. Energy 41 (19), 7732–7743. http://dx.doi.org/10.1016/j.ijhydene.2016.01.113.

Fleck, B., Huot, M., 2009. Comparative life-cycle assessment of a small wind turbine for residential off-grid use. Renew. Energy 34 (12), 2688–2696. http://dx.doi.org/10.1016/j.renene.2009.06.016.

Gracia, L., Casero, P., Bourasseau, C., Chabert, A., 2018. Use of hydrogen in off-grid locations, a techno-economic assessment. Energies 11 (11), 3141. http://dx.doi.org/10.3390/en11113141.

Groppi, D., Astiaso Garcia, D., Lo Basso, G., Cumo, F., De Santoli, L., 2018. Analysing economic and environmental sustainability related to the use of battery and hydrogen energy storages for increasing the energy independence of small islands. Energy Convers. Manage. 177 (September), 64–76. http://dx.doi.org/10.1016/j.enconman.2018.09.063.

Guinot, B., et al., 2015. Techno-economic study of a PV-hydrogen-battery hybrid system for off-grid power supply: Impact of performances' ageing on optimal system sizing and competitiveness. Int. J. Hydrog. Energy 40 (1), 623–632. http://dx.doi.org/10.1016/j.ijhydene.2014.11.007.

Gutiérrez-Martín, F., Amodio, L., Pagano, M., 2021. Hydrogen production by water electrolysis and off-grid solar PV. Int. J. Hydrog. Energy 46 (57), 29038–29048. http://dx.doi.org/10.1016/j.ijhydene.2020.09.098.

Hiremath, M., Derendorf, K., Vogt, T., 2015. Comparative life cycle assessment of battery storage systems for stationary applications. Environ. Sci. Technol. 49 (8), 4825–4833. http://dx.doi.org/10.1021/es504572q.

Homayouni, F., Roshandel, R., Hamidi, A.A., 2017. Sizing and performance analysis of standalone hybrid photovoltaic/battery/hydrogen storage technology power generation systems based on the energy hub concept. Int. J. Green Energy 14 (2), 121–134. http://dx.doi.org/10.1080/15435075.2016.1233423.

Honny Power, 2021. HGM138 google diesel generator. [Online]. Available: http://www.honnypower.com/20_250kW/show/25.html [Accessed: 04-Oct-2021].

International Energy Agency, 2021. Global hydrogen review 2021.

IPCC - The Intergovernmental Panel on Climate Change, 2014. Climate Change 2014. Synthesis Report.

IRENA, 2015. Off-grid renewable energy systems: status and methodological issues.

2006a. UNI EN ISO 14040: 2006. Environmental Management - Life Cycle Assessment - Principles and Framework. ISO - International Organization for Standardization.

2006b. UNI EN ISO 14044: 2006. Environmental Management - Life Cycle Assessment - Requirements and Guidelines. ISO - International Organization for Standardization.

2015. ISSF - international stainless steel forum, stainless steel and CO2: Facts and scientific observations. [Online]. Available: https://aceroplatea.es/docs/ISSF_Stainless_Steel_{and}_CO2.pdf [Accessed: 04-Oct-2021].

Jakhrani, A.Q., Rigit, A.R.H., Othman, A.K., Samo, S.R., Kamboh, S.A., 2012. Estimation of carbon footprints from diesel generator emissions. In: Proceedings of the 2012 International Conference in Green and Ubiquitous Technology, GUT 2012. pp. 78–81. http://dx.doi.org/10.1109/GUT.2012.6344193.

Janssen, J.L.L.C.C., Weeda, M., Detz, R.J., van der Zwaan, B., 2022. Country-specific cost projections for renewable hydrogen production through off-grid electricity systems. Appl. Energy 309 (2021), 118398. http://dx.doi.org/10.1016/j.apenergy.2021.118398.

Karlsdóttir, S.H., 2013. Experience in Transporting Energy Through Subsea Power Cables: The Case of Iceland. University of Iceland.

Kaut, M., Flatberg, T., Muñoz-Ortiz, M., 2020. The HyOpt model input data and mathematical formulation.

Kohler, 2021. KD66 w kohler diesel generator. [Online]. Available: www.KohlerPower.com [Accessed: 04-Oct-2021].

Ludin, N.A., et al., 2018. Prospects of life cycle assessment of renewable energy from solar photovoltaic technologies: A review. Renew. Sustain. Energy Rev. 96 (2017), 11–28. http://dx.doi.org/10.1016/j.rser.2018.07.048.

Luo, X., Wang, J., Dooner, M., Clarke, J., 2015. Overview of current development in electrical energy storage technologies and the application potential in power system operation. Appl. Energy 137, 511–536. http://dx.doi.org/10.1016/j.apenergy.2014.09.081.

Magrassi, F., Rocco, E., Barberis, S., Gallo, M., Del Borghi, A., 2019. Hybrid solar power system versus photovoltaic plant: A comparative analysis through a life cycle approach. Renew. Energy 130, 290–304. http://dx.doi.org/10.1016/j.renene.2018.06.072.

Marchenko, O.V., Solomin, S.V., 2017. Modeling of hydrogen and electrical energy storages in wind/PV energy system on the lake baikal coast. Int. J. Hydrog. Energy 42 (15), 9361–9370. http://dx.doi.org/10.1016/j.ijhydene.2017.02.076.

Margaret Amutha, W., Rajini, V., 2015. Techno-economic evaluation of various hybrid power systems for rural telecom. Renew. Sustain. Energy Rev. 43, 553–561. http://dx.doi.org/10.1016/j.rser.2014.10.103.

Marocco, P., Ferrero, D., Gandiglio, M., Santarelli, M., 2018. Deliverable number 2.2. Technical specification of the technological demonstrators.

Marocco, P., Ferrero, D., Lanzini, A., Santarelli, M., 2021a. Optimal design of stand-alone solutions based on RES + hydrogen storage feeding off-grid communities. Energy Convers. Manage. 238, 114147. http://dx.doi.org/10.1016/j.enconman.2021.114147.

Marocco, P., Ferrero, D., Martelli, E., Santarelli, M., Lanzini, A., 2021b. An MILP approach for the optimal design of renewable battery-hydrogen energy systems for off-grid insular communities. Energy Convers. Manage. 245, 114564. http://dx.doi.org/10.1016/j.enconman.2021.114564.

Marocco, P., et al., 2020. A study of the techno-economic feasibility of H2-based energy storage systems in remote areas. Energy Convers. Manage. 211, 112768. http://dx.doi.org/10.1016/j.enconman.2020.112768.

Mori, M., Jensterle, M., Mržljak, T., Drobnič, B., 2014. Life-cycle assessment of a hydrogen-based uninterruptible power supply system using renewable energy. Int. J. Life Cycle Assess. 19 (11), 1810–1822. http://dx.doi.org/10.1007/s11367-014-0790-6.

Moro, A., Lonza, L., 2018. Electricity carbon intensity in European member states: Impacts on GHG emissions of electric vehicles. Transp. Res. D 64 (2017), 5–14. http://dx.doi.org/10.1016/j.trd.2017.07.012.

Nexans, 2021. Datasheet of the submarine cable 2XS(FL)2YRAA 3x1x70 RM/16 6/10 (12)kV. [Online]. Available: https://www.nexans.com [Accessed: 17-Oct-2021].

Nian, V., Liu, Y., Zhong, S., 2019. Life cycle cost–benefit analysis of offshore wind energy under the climatic conditions in southeast Asia – setting the bottom-line for deployment. Appl. Energy 233–234 (2018), 1003–1014. http://dx.doi.org/10.1016/j.apenergy.2018.10.042.

NVE, 2021. Official website of the Norwegian water resources and energy directorate (NVE). [Online]. Available: https://www.nve.no/ [Accessed: 04-Oct-2021].

Proost, J., 2019. State-of-the art CAPEX data for water electrolysers, and their impact on renewable hydrogen price settings. Int. J. Hydrog. Energy 44 (9), 4406–4413. http://dx.doi.org/10.1016/j.ijhydene.2018.07.164.

Raadal, H.L., Gagnon, L., Modahl, I.S., Hanssen, O.J., 2011. Life cycle greenhouse gas (GHG) emissions from the generation of wind and hydro power. Renew. Sustain. Energy Rev. 15 (7), 3417–3422. http://dx.doi.org/10.1016/j.rser.2011.05.001.

2018. REMOTE project official website. [Online]. Available: https://www.remote-euproject.eu/ [Accessed: 30-May-2021].

Roy, S., Das, R., Saha, U.K., 2018. An inverse method for optimization of geometric parameters of a savonius-style wind turbine. Energy Convers. Manage. 155 (2017), 116–127. http://dx.doi.org/10.1016/j.enconman.2017.10.088.

Sawle, Y., Gupta, S.C., Bohre, A.K., 2018. Review of hybrid renewable energy systems with comparative analysis of off-grid hybrid system. Renew. Sustain. Energy Rev. 81 (2017), 2217–2235. http://dx.doi.org/10.1016/j.rser.2017.06.033.

Shahid, Z., Santarelli, M., Marocco, P., Ferrero, D., Zahid, U., 2022. Techno-economic feasibility analysis of renewable-fed power-to-power (P2P) systems for small French islands. Energy Convers. Manage. 255, 115368. http://dx.doi.org/10.1016/j.enconman.2022.115368.

Shehzad, M.F., Abdelghany, M.B., Liuzza, D., Mariani, V., Glielmo, L., 2019. Mixed logic dynamic models for MPC control of wind farm hydrogen-based storage systems. Inventions 4 (4), 1–17. http://dx.doi.org/10.3390/inventions4040057.

SINTEF, 2022. SINTEF website. [Online]. Available: https://www.sintef.no/en/ [Accessed: 22-Feb-2022].

Smith, C., et al., 2015. Comparative life cycle assessment of a Thai island's diesel/PV/wind hybrid microgrid. Renew. Energy 80, 85–100. http://dx.doi.org/10.1016/j.renene.2015.01.003.

Stropnik, R., Sekavčnik, M., Ferriz, A.M., Mori, M., 2018. Reducing environmental impacts of the ups system based on PEM fuel cell with circular economy. Energy 165, 824–835. http://dx.doi.org/10.1016/j.energy.2018.09.201.

The Wind Power, 2021. Vestas V27/225. [Online]. Available: https://www.thewindpower.net/turbine_en_208_vestas_v27-225.php [Accessed: 09-Oct-2021].

Tractebel, Hinicio, 2017. Study on early business cases for H2 in energy storage and more broadly power to H2 applications.

TrønderEnergi, 2021. TrønderEnergi web site. [Online]. Available: https://tronderenergi.no/ [Accessed: 29-Oct-2021].

Tsiropoulos, I., Tarvydas, D., Lebedeva, N., 2018. Li-ion batteries for mobility and stationary storage applications.

Vandepaer, L., Cloutier, J., Amor, B., 2017. Environmental impacts of lithium metal polymer and lithium-ion stationary batteries. Renew. Sustain. Energy Rev. 78 (April), 46–60. http://dx.doi.org/10.1016/j.rser.2017.04.057.

Varun, Bhat, I.K., Prakash, R., 2009. LCA of renewable energy for electricity generation systems-a review. Renew. Sustain. Energy Rev. 13 (5), 1067–1073. http://dx.doi.org/10.1016/j.rser.2008.08.004.

Verma, S., Das, R., 2021. Performance analysis of a solar still driven by a packed bed thermal storage tank during off-sunshine period. J. Energy Storage 44 (PA), 103381. http://dx.doi.org/10.1016/j.est.2021.103381.

Vivas, F.J., De las Heras, A., Segura, F., Andújar, J.M., 2018. A review of energy management strategies for renewable hybrid energy systems with hydrogen backup. Renew. Sustain. Energy Rev. 82 (Part 1), 126–155. http://dx.doi.org/10.1016/j.rser.2017.09.014.

Wang, Y., Sun, T., 2012. Life cycle assessment of CO 2 emissions from wind power plants: Methodology and case studies. Renew. Energy 43 (2012), 30–36. http://dx.doi.org/10.1016/j.renene.2011.12.017.

Wang, Q., et al., 2018. Environmental impact analysis and process optimization of batteries based on life cycle assessment. J. Clean. Prod. 174, 1262–1273. http://dx.doi.org/10.1016/j.jclepro.2017.11.059.

Warnock, J., McMillan, D., Pilgrim, J., Shenton, S., 2019. Failure rates of offshore wind transmission systems. Energies 12 (14), 1–12. http://dx.doi.org/10.3390/en12142682.

Yang, J., Chang, Y., Zhang, L., Hao, Y., Yan, Q., Wang, C., 2018. The life-cycle energy and environmental emissions of a typical offshore wind farm in China. J. Clean. Prod. 180, 316–324. http://dx.doi.org/10.1016/j.jclepro.2018.01.082.

Zhang, X., Bauer, C., Mutel, C.L., Volkart, K., 2017. Life cycle assessment of power-to-gas: Approaches, system variations and their environmental implications. Appl. Energy 190, 326–338. http://dx.doi.org/10.1016/j.apenergy.2016.12.098.

Zhao, G., Nielsen, E.R., Troncoso, E., Hyde, K., Romeo, J.S., Diderich, M., 2019. Life cycle cost analysis: A case study of hydrogen energy application on the Orkney islands. Int. J. Hydrog. Energy 9517–9528. http://dx.doi.org/10.1016/j.ijhydene.2018.08.015.

Zhao, G., Pedersen, A.S., 2018. Life cycle assessment of hydrogen production and consumption in an isolated territory. Procedia CIRP 69, 529–533. http://dx.doi.org/10.1016/j.procir.2017.11.100.